THE JOURNAL OF PHYSICAL CHEMISTRY A

Article

pubs.acs.org/JPCA

Fluorescent Ligands and Energy Transfer in Photoactive Ruthenium–Bipyridine Complexes

Guillermo Carrone, Federico Gantov, Leonardo D. Slep, and Roberto Etchenique*

Departamento de Química Inorgánica, Analítica y Química Física, INQUIMAE, Facultad de Ciencias Exactas y Naturales, Universidad de Buenos Aires, Ciudad Universitaria Pabellón 2, AR1428EHA Buenos Aires, Argentina

Supporting Information

ABSTRACT: Ruthenium bis(bipyridine) complexes have proved to be useful as phototriggers for visible and IR-light photodelivery of molecules. They usually expel one ligand heterolytically upon absorption of blue or green light. However, their absorption capabilities at wavelengths longer than 500 nm are poor. Through coordination of fluorescent ligands to the Ru center, it is possible to establish an energy transfer pathway that allows these kinds of complexes to extend the range of photoactivation up to yellow wavelengths. We introduce a study of this effect in several complexes of the family using a modified Rhodamine as fluorescent ligand with different coordinated linkers. The observed trends show that a rational design of fluorophore-enhanced Ru-bpy phototriggers is possible and that photolysis efficiency can be increased by choosing the right combination of ligands.

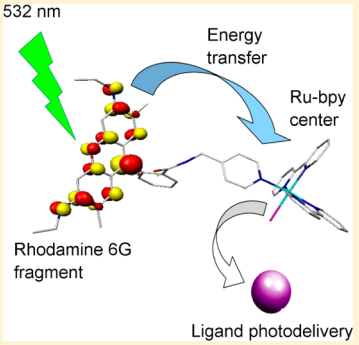

INTRODUCTION

The photochemistry of ruthenium(II) polypyridines constitutes the base of several molecular systems. Among them, the collection of solar energy[1−5] and the photodelivery of biomolecules and drugs[6−15] are two of the more promising applications.

One of the more profusely studied polypyridines, the complexes of the form $[Ru(bpy)_2L_1L_2]^{n+}$ (bpy = 2,2′ bipyridine), from now on called "Ru-bpy", present a very interesting photochemistry: Irradiation of a Ru(II)→ π^*_{bpy} ^{1}MLCT band (located usually in the blue range of the spectrum) populates this excited state, which decays to a rather long-lived ^{3}MLCT. From this triplet a nearby ^{3}MC dissociative state becomes thermally accessible, usually yielding a free monodentate ligand and a Ru-bpy aquo or solvento complex.[16−19] Being an activated pathway, the energy difference between the MLCT states and the ^{3}MC state determines the efficiency of the photolysis. Pinnick and Durham[16,17] demonstrated a strong correlation between the ^{1}MLCT band position and the quantum yield of photoaquation. This fact implies that although it is possible to tune the MLCT band to be absorptive in the green or yellow region of the spectrum by changing the ligands, the obtained complex will have a very low photolysis quantum yield.

Caged compounds, molecules that can release a fragment that has biological activity, constitute important tools in the field of cellular physiology.[20−22] Traditional caged compounds, based on organic photoprotective groups, need a pulse of UV light to release the desired biomolecule.[23−25] The use of UV light on biological systems not only introduces a potentially deleterious perturbation but also generates two-sided problems: the need of expensive quartz optics and the low penetration depth of short-wavelength light. Scattering in biological tissues is a big issue, and it scales with the fourth power of the photon frequency.[26] Thus, a 532 nm (green) photon has a penetrance about 5 times deeper than a 360 nm (UV) photon. Ru-bpy caged compounds can be triggered with blue light, and their absorption extends to the green region (540 nm). However, for any Ru-bpy complex with high enough photorelease quantum yield the absorption at these long wavelengths is low, implying that high concentrations of the complex and/or high light intensities will be mandatory for many applications. In brief, long wavelength absorption comes with low efficiency.

In recent works it was shown that it is possible to avoid this problem by means of a different approach: keeping the absorption band in the blue region, guaranteeing a high quantum yield of photolysis and using a coordinant fluorophore as ligand, with high absorptivity at long wavelengths and high emission quantum yield. The first report of such a compound was $[Ru(bpy)_2Cl(RhodB\text{-}MAPN)]^+$ (RhodB-MAPN = RhodamineB-methylaminopropionitrileamide), which releases the fluorescent ligand RhodB-MAPN upon irradiation with green light, enhancing the photoprocess efficiency up to 24 times with respect to an analogue complex lacking the fluorophore.[27] The next step was done recently by Bonnet et al.[28] using the slightly different complex $[Ru(bpy)(tpy\text{-}Rhod)(Hmte)]^{2+}$ (tpy-Rhod = 2,2′;6′,2″-terpyridine, 4′ *N*-methyl RhodamineB-amide ethyl ether; Hmte = 2-(methylthio)ethanol) who demonstrate that it is possible to release a monodentate ligand by irradiation on the band of the Rhodamine-modified terpyridine. The quantum

Special Issue: Current Topics in Photochemistry

Received: April 24, 2014
Revised: July 10, 2014

   dx.doi.org/10.1021/jp504030f | *J. Phys. Chem. A* XXXX, XXX, XXX−XXX

yield of photorelease is almost invariant with the wavelength, extending the activity of the Ru complex to the yellow region.

Both findings suggest that the position of the fluorescent ligand and its exact distance to the Ru center can be varied without loss of the energy-scavenge properties, and that a family of different Ru-bpy complexes having fluorophore-enhanced photoactivity can be produced. In this article, we start this work with a systematic study of the photophysical and photochemical properties of complexes of the form $[Ru(bpy)_2(F)(L)]^{n+}$, with F being a fluorescent molecule, modified to allow coordination to Ru, and L being a nonfluorescent ligand.

EXPERIMENTAL SECTION

All reagents were commercially available and used as received. $Ru(bpy)_2Cl_2$ was synthesized according to the literature.[29] UV−vis and fluorescence spectra were taken with a Ocean Optics Chem2000 spectrophotometer. NMR spectra were obtained using a 500 MHz Bruker AM-500. Visible light irradiation of samples was performed with laser diodes of 405 and 445 nm and a Diode Pumped NdYAG doubled at 532 nm. All syntheses were done by degassing the solutions with either Ar or N_2 prior to heating to prevent oxidation of the Ruthenium aquo complexes.

Syntheses. *$[Ru(bpy)_2(L)Cl]Cl$ for L = Rhod6G-4Pic, Rhod6G-1,3DAP, and Rhod6G-1,2DAE.* One hundred milligrams of $Ru(bpy)_2Cl_2$ was dissolved in 10 mL of methanol and refluxed for 3 h to form $[Ru(bpy)_2(H_2O)Cl]^+$. The solution was filtered to remove any solids and 1.1 mol equiv of the corresponding ligand was added. The solution was heated at 60 °C in a water bath. The formation of the complex $[Ru(bpy)_2(L)Cl]^+$ was determined by UV−vis spectroscopy. After 2 h, no further changes were observed and the spectra corresponded to that of the desired complex. The solution was evaporated at reduced pressure until minimum volume and 2−3 mL of acetone was added. After cooling to RT, the complex was precipitated by the addition of diethyl ether under continuous stirring. It was washed several times with diethyl ether and dried protected from the light.

L = Rhod6G-4Pic ^{1}H NMR ($CDCl_3$) δ 1.32 (t, 3H, J = 7.2 Hz), 1.34 (t, 3H, J = 7.2 Hz), 3.21 (m, 4H), 3.50 (d, 2H, J = 5.1 Hz), 3.76 (m, 2H), 4.08 (d, 1H, J = 15.7 Hz), 4.19 (d, 1H, J = 15.7 Hz), 5.97 (s, 1H), 6.02 (s, 1H), 6.26 (s, 1H), 3.3 (s, 1H), 6.77 (d, 2H, J = 6.6 Hz), 7.07 (m, 1H), 7.12 (t, 1H, J = 6.6 Hz), 7.29 (t, 1H, J = 7.6 Hz), 7.48 (m, 2H), 7.52 (d, 1H, J = 5.7 Hz), 7.55 (t, 1H, J = 7.6 Hz), 7.62 (t, 1H, J = 5.7 Hz), 7.63 (d, 1H, J = Hz), 7.75 (t, 1H, J = 7.6 Hz), 7.91 (m, 2H), 8.05 (t, 1H, J = 7.6 Hz), 8.10 (t, 1H, J = 7.6 Hz), 8.30 (d, 1H, J = 7.6 Hz), 8.38 (d, 1H, J = 5.7 Hz), 8.46 (d, 1H, J = 7.6 Hz), 8.95 (d, 1H, J = 7.6 Hz), 8.99 (d, 1H, J = 7.6 Hz), 9.91 (d, 1H, J = 5.7 Hz).

L = Rhod6G-1,2DAE ^{1}H NMR ($CDCl_3$) δ 1.33 (t, 3H, J = 7.2 Hz), 1.36 (t, 3H, J = 7.2 Hz), 1.87 (s, 3H), 1.95 (s, 3H), 2.86 (m, 1H), 3.06 (m, 1H), 3.22 (m, 6H), 3.55 (t, 1H, J = 11.7 Hz), 3.93 (t, 1H, J = 11.7 Hz), 5.97 (s, 1H), 6.17 (s, 1H), 6.27 (s, 1H), 6.28 (s, 1H), 6.99 (t, 1H, J = 6.9 Hz), 7.01 (m, 1H), 7.12 (t, 1H, J = 6.5 Hz), 7.33 (d, 1H, J = 6.0 Hz), 7.46 (m, 2H), 7.53 (t, 1H, J = 6.2 Hz), 7.62 (t, 1H, J = 8.0 Hz), 7.69 (d, 1H, J = 5.7 Hz), 7.76 (t, 1H, J = 8.0 Hz), 7.78 (t, 1H, J = 7.0 Hz), 7.86 (m, 1H), 8.01 (t, 1H, J = 8.0 Hz), 8.09 (t, 1H, J = 8.0 Hz), 8.15 (d, 1H, J = 8.0 Hz), 8.33 (d, 1H, J = 8.0 Hz), 8.76 (d, 1H, J = 8.0 Hz), 8.91 (d, 1H, J = 8.0 Hz), 9.25 (d, 1H, J = 5.7 Hz), 9.74 (d, 1H, J = 5.2 Hz).

L = Rhod6G-1,3DAP ^{1}H NMR ($CDCl_3$) δ 1.06 (m, 3H), 1.25 (t, 3H, J = 6.9 Hz), 1.31 (t, 3H, J = 7.3 Hz), 1.8 (s, 3H), 1.82 (s, 3H), 2.83 (dt, 1H, J = 15.1, 4.5 Hz), 3.18 (m, 4H), 3.27 (t, 1H, J = Hz), 3.42 (m, 1H, J = Hz), 3.53 (br s., 1H), 3.60 (br s., 1H), 3.71 (d, 1H, J = 7.1 Hz), 3.74 (d, 1H, J = 7.1 Hz), 4.86 (br t., 1H, J = 10.4 Hz), 5.61 (s, 1H), 5.91 (s, 1H), 6.23 (s, 1H), 6.29 (s, 1H), 7.00 (d, 1H, J = 7.8 Hz), 7.03 (t, 1H, J = 6.7 Hz), 7.15 (t, 1H, J = 7.2 Hz), 7.33 (d, 1H, J = 5.5 Hz), 7.49 (m, 2H), 7.65 (m, 2H), 7.69 (d, 1H, J = 7.6 Hz), 7.77 (t, 1H, J = 8.2 Hz), 7.80 (t, 1H, J = 5.5 Hz), 7.98 (d, 1H, J = 5.5 Hz), 8.03 (t, 1H, J = 8.2 Hz), 8.14 (d, 1H, J = 8.2 Hz), 8.20 (t, 1H, J = 8.2 Hz), 8.32 (d, 1H, J = 8.2 Hz), 8.93 (d, 1H, J = 8.2 Hz), 9.13 (d, 1H, J = 8.2 Hz), 9.54 (d, 1H, J = 5.5 Hz), 9.97 (d, 1H, J = 5.5 Hz).

$[Ru(bpy)_2(4PAA)Cl]PF_6$. One hundred milligrams of $Ru(bpy)_2Cl_2$ was dissolved in 10 mL of methanol and refluxed for 3 h to form $[Ru(bpy)_2(H_2O)Cl]^+$. The solution was filtered to remove any solids, and 1.1 mol equiv of the corresponding ligand was added. The solution was heated at 60 °C in a water bath. The formation of the complex $[Ru(bpy)_2(L)Cl]^+$ was determined by UV−vis. After 2 h, no further changes were observed, and the spectra corresponded to that of the desired complex. The mixture was evaporated at reduced pressure until 0.5 mL, water (5 mL) was added, and the solution was precipitated with an excess of a 0.5 M solution of KPF_6 in water. The solid was washed several times with cold water and dried. ^{1}H NMR (acetone-d_6) δ 1.93 (s, 3H), 4.35 (d, 1H, J = 15.2 Hz), 4.40 (d, 1H, J = 15.2 Hz), 7.24 (d, 2H, J = 6.5 Hz), 7.29 (t, 1H, J = 6.5 Hz), 7.37 (t, 1H, J = 7.1 Hz), 7.63 (br s., 2H), 7.71 (t, 1H, J = 6.5 Hz), 7.77 (d, 1H, J = 5.5 Hz), 7.88 (t, 1H, J = 6.7 Hz), 7.90 (t, 1H, J = 7.3 Hz), 7.92 (t, 1H, J = 7.4 Hz), 8.10 (d, 1H, J = 5.8 Hz), 8.18 (t, 2H, J = 7.8 Hz), 8.55 (d, 1H, J = 7.8 Hz), 8.59 (d, 1H, J = 7.8 Hz), 8.62 (d, 1H, J = 7.8 Hz), 8.66 (d, 1H, J = 5.5 Hz), 8.72 (d, 1H, J = 7.8 Hz), 10.06 (d, 1H, J = 5.5 Hz).

Rhod6G-4Pic. Eighty milligrams of Rhodamine 6G was dissolved in 2 mL of dry DMF. Forty microliters of 4-pycolylamine was added and the solution stirred at 50 °C during 48 h. The ligand was precipitated by pouring the solution over 20 mL of water at 0 °C. ^{1}H NMR ($CDCl_3$) δ 1.33 (t, 3H, J = 7.0 Hz), 1.76 (s, 6H), 3.20 (q, 4H, J = 7.0 Hz), 3.47 (broad s., 2H), 4.27 (s, 2H), 5.99 (s, 2H), 6.27 (s, 2H), 6.90 (d, 2H, J = 6.0 Hz), 7.08 (d, 1H, J = 7.0 Hz), 7.49 (m, 2H), 7.99 (d, 1H, J = 7.0 Hz), 8.16 (d, 2H, J = 5.6 Hz). Yield 67%.

Rhod6G-1,2DAE. The same procedure was followed, but 1,2 diaminoethane was used instead of 4-pycolylamine. ^{1}H NMR ($CDCl_3$) δ 1.33 (t, 6H, J = 7.2 Hz), 1.91 (s, 6H), 2.37 (t, 2H, J = 6.8 Hz), 3.17 (t, 2H, J = 6.8 Hz), 3.21 (m, 4H), 3.51 (broad s., 2H), 6.23 (s, 2H), 6.35 (s, 2H), 7.06 (d, 1H, J = 5.2 Hz), 7.47 (m, 2H), 7.93 (d, 1H, J = 5.2 Hz). Yield 65%.

Rhod6G-1,3DAP. The same procedure was followed, but 1,3 diaminopropane was used instead of 4-pycolylamine. ^{1}H NMR ($CDCl_3$) δ 1.17 (m, 2H), 1.33 (t, 6H, J = 7.2 Hz), 1.90 (s, 6H), 2.46 (t, 2H, J = 6.3 Hz), 3.20 (t, 2H, J = 6.9 Hz), 3.21 (m, 4H,), 3.5 (broad t., 2H, J = 4.8 Hz), 6.22 (s, 2H), 6.35 (s, 2H), 7.05 (d, 1H, J = 7.2 Hz), 7.45 (m, 2H), 7.9 (d, 1H, J = 7.2 Hz). Yield 61%.

4PAA. Two hundred microliters of 4-picolylamine was stirred in a test tube. Two hundred and fifty microliters of acetic anhydride was added; the mixture increased its temperature and turned brownish. After 10 min, 2 mL of methanol was added and dried under reduced pressure at RT in a rotary evaporator. The solid was extracted with CH_2Cl_2 from H_2O three times. The three organic phases were combined and dried. ^{1}H NMR

dx.doi.org/10.1021/jp504030f | J. Phys. Chem. A XXXX, XXX, XXX−XXX

($CDCl_3$) δ 2.09 (s, 3H), 4.46 (d, 2H, J = 6.0 Hz), 5.98 (broad s, 1H), 7.20 (d, 2H, J = 5.8 Hz), 8.56 (d, 2H, J = 5.8 Hz). Yield 55%.

DFT Computational Details. We employed density functional theory (DFT) computations to fully optimize the ground-state geometries of all the species described in this work. The calculations were done with Gaussian 09[30] using Becke's three parameter hybrid functional with the correlation functional of Lee, Yang, and Parr formalized as the B3LYP hybrid functional[31−34] and the effective core potential basis set LanL2DZ,[35−38] which proved to be suitable for geometry predictions in coordination compounds containing metals of the second row of the transition elements in the periodic table. We used tight SCF convergence criteria and default setting in the geometry optimizations. The nature of the resulting stationary points was in all cases tested by computing the vibrational spectrum.

The analysis of the electronic structure was complemented with time-dependent (TD)DFT computations including up to 100 states of the same multiplicity as the ground state for $[Ru(bpy)_2pyCl]^+$ (py = pyridine) and 200 states for $[Ru(bpy)_2(Rhod6G\text{-}4Pic)Cl]^{2+}$. The molecular orbital picture as well as the electronic spectra were computed at the gas phase geometry of each species, though solvation effects in solution (a mixture of ethanol and water) were introduced employing the PCM approximation, as implemented in Gaussian 09.[30]

RESULTS AND DISCUSSION

With a few exceptions, fluorescent molecules are not good ligands for Ru(II) complexes. In particular, Ru-bpy complexes establish strong coordination with aliphatic amines, imines, pyridines, nitriles, thiolates, thioethers, phosphines and other sulfur and phosphorus derivatives. However, carboxylates, anilines, and phenolates, which often are present in fluorescent molecules, are easily displaced by water as ligands even at room temperature. Because of this fact, the first step to develop a fluorophore capable to act as a ligand in a Ru-bpy complex implies a chemical derivatization.

Reverse FRET[39] is probably the key mechanism by which fluorescent rhodamines transfer the captured energy to Ru-bpy centers.[27,28] For the energy transfer to be possible, some overlap between the emission spectrum of the ligand and the absorption band of the Ru-bpy ^{1}MLCT band must be present. Rhodamines are a good choice for antenna-ligands since they present a variety of types, each with somewhat different photophysical properties, at a time that they present a carboxylate group that can be used for derivatization to form a coordinating moiety without interfering with its emission capabilities.

Analysis of the energy transfer implies that both the emission of the ligand and the absorption of the Ru-bpy center must be measured independently. The fact that the molar absorptivity of the fluorescent ligand is usually an order of magnitude higher that that of the ^{1}MLCT Ru-bpy band makes it difficult to properly measure the absorption. One possibility to circumvent this problem consists in using an analogue complex, bearing a ligand that resembles the fluorophore coordination but with no absorption.[27,28] Although we have used this approach for comparison, a new strategy is presented, which involves conformational change of the emissive ligands to "switch off" its absorption (and emission) in a reversible way.

Figure 1a shows the structures of Rhodamine 6G and its derivatives Rhod6G-4Pic, Rhod6G-1,2DAE, and Rhod6G-1,3DAP. In every case, an amide bond is formed between the benzoic moiety of the Rhodamine and the amine group of 4-picolylamine (4Pic), 1,2-diaminoethane (1,2DAE) or 1,3-diaminopropane (1,3DAP), respectively. This reaction is very simple and efficient and has been proved for a number of primary amines.[40]

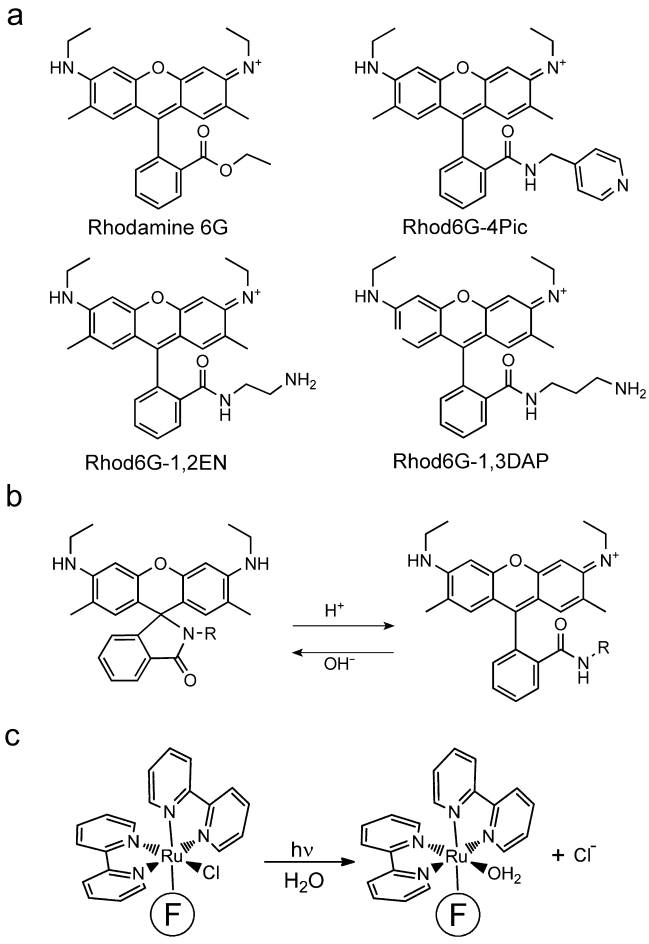

Figure 1. (a) Structure of the fluorescent ligands used in this work. The names given are generic and correspond to the basic form, although the structures are depicted in its acid form, which are more informative. (b) Acid−base equilibrium of Rhodamine amides. (c) Structure of the complexes bearing the fluorescent ligands and the studied photoreaction.

The synthesized Rhodamine amides can exist in two main forms: a fluorescent, open form and a nonabsorptive, nonfluorescent closed spirolactam. The switching between these two forms depends on the solvent and on the acidity of the medium (Figure 1b). In aqueous solution the spirolactam is the prevalent species at pH > 5. In EtOH/H_2O 70:30 v/v solutions, the open fluorescent form can be easily formed by adding a strong acid to 10 mM. While the conversion from the spirolactam to the open form takes several minutes after acid addition, the reversion to the nonfluorescent form by adding a base appears as instantaneous at the UV−vis measurement time scale.

This behavior allowed us to measure the absorption of both the Rhodamine and the ^{1}MLCT band of the Ru-bpy core by adjusting the acidity of the medium.

Figure 1c shows the general structure of the studied complexes: the two bipyridines are in cis position, and the

dx.doi.org/10.1021/jp504030f | J. Phys. Chem. A XXXX, XXX, XXX−XXX

fluorescent ligands are coordinated by the basic nitrogens of the linkers (pyridinic or aliphatic).

The complex *cis*$[Ru(bpy)_2(Rhod6G\text{-}4Pic)Cl]^+$ can be obtained by heating a methanolic solution of the precursor *cis*-$[Ru(bpy)_2(H_2O)Cl]^+$ with a little excess of Rhod6G-4Pic and further purification (see experimental section). The product can be used directly as a model for photolysis. Figure 2 shows the UV−vis spectrum of the complex $[Ru(bpy)_2(Rhod6G\text{-}4Pic)Cl]^+$ in a $EtOH/H_2O$ 70:30 v/v solution. The ^{1}MLCT band presents a maximum at 495 nm with ε = 10400 M^{-1} cm^{-1}. After the addition of a drop of HCl(c), the band corresponding to the open (acid) form of H-Rhod6G-4Pic starts to grow. After 20 min in darkness, the spectrum shows the characteristic maximum of Rhodamine at 534 nm. The fluorescence spectrum of H-Rhod6G-4Pic is almost indistinguishable from that of Rhodamine 6G. Its quantum efficiency was measured using Rhodamine 6G as a standard[41] (ϕ_F = 0.95) and resulted to be also 0.95 within the uncertainty of the measurement (1%).

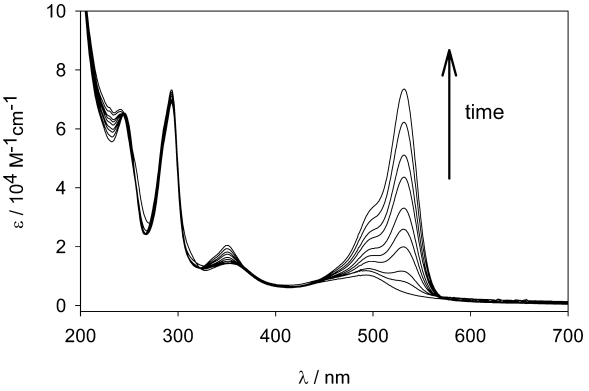

Figure 2. Absorption spectra of a solution of $[Ru(bpy)_2(Rhod6G\text{-}4Pic)Cl]^+$ in $EtOH/H_2O$ 70:30 v/v after acidification with HCl(c). After 20 min the ligand H-Rhod6G-4Pic is completely in its open form, showing a high absorption at 534 nm.

The high fluorescence of H-Rhod6G-4Pic drops dramatically after coordination to the Ru-bpy center to form $[Ru(bpy)_2(H\text{-}Rhod6G\text{-}4Pic)Cl]^{2+}$. Its fluorescent quantum yield changes from ϕ_F = 0.95 to ϕ_F = 0.02. When a solution of the complex is irradiated with 400−550 nm light the fluorescence increases with time, as can be seen in Figure 3.

This photolysis shows two processes with very different time constants (at constant light power, it means two different photolysis efficiencies). The fitting of the whole curve allows the determination of the quantum yields of the two processes: $\phi_{1P} = 9 \times 10^{-3}$ and $\phi_{2P} = 1.7 \times 10^{-5}$. The UV−vis spectra of the formed species after the first photoprocess is almost complete shows that the first process involves the release of chloride to form the aqua complex $[Ru(bpy)_2(H\text{-}Rhod6G\text{-}4Pic)(H_2O)]^{3+}$. In this complex the overlap between Rhod emission and ^{1}MLCT Ru absorption is somewhat lower due to the UV-shift of the latter band, and therefore, some increase in fluorescence is expected. The second process, which accounts for the 94% of the increment in fluorescence, corresponds to the photouncaging of H-Rhod6G-4Pic yielding the free ligand and $[Ru(bpy)_2(H_2O)_2]^{2+}$. The extremely low efficiency of this second photoreaction implies that the separation of both processes is very easy and that the coordination bond between Ru and Rhod6G-4Pic can be regarded in our time scales as stable ($t_{1/2} \approx$ 2.7 h under 10 mW irradiation).

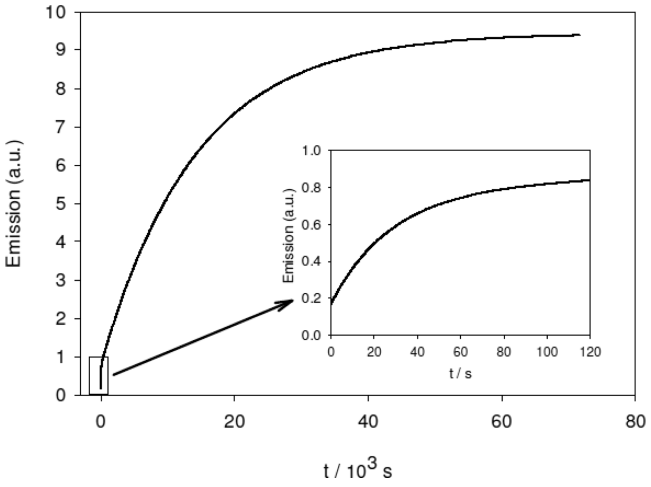

Figure 3. Fluorescent emission of a solution of $[Ru(bpy)_2(H\text{-}Rhod6G\text{-}4Pic)Cl]^{2+}$ $EtOH/H_2O$ 70:30 v/v acidified with HTos (*p*-toluenesulfonic acid) during photolysis at 532 nm. Inset: Enlarged plot of the first 120 s showing the first photoprocess. λ_{exc} = 532 nm, λ_{em} = 550 nm, and $c_{Ru} = 2 \times 10^{-5}$ M.

Once determined that the two photoprocesses can be separated, a complete study of the first photoaquation was conducted in neutral and acidic media. The photolysis of solutions of $[Ru(bpy)_2(Rhod6G\text{-}4Pic)Cl]^+$ in neutral $EtOH/H_2O$ 70:30 v/v to yield $[Ru(bpy)_2(Rhod6G\text{-}4Pic)(H_2O)]^{2+}$ during irradiation at three different wavelengths is depicted in Figure 4a. Besides 532 nm, which corresponds to the second harmonic Nd:YAG laser, the two wavelengths of the widely used solid-state laser diodes, 445 and 405 nm were used. This election corresponds not only to the main activity range of the studied compounds but also to the cheapest options available for any low-power laser application. The inset shows a subset of spectra obtained. The isosbestic point shows that just one colored product is formed: the aqua complex at 476 nm that appears at the expense of the initial band, corresponding to the chlorido complex. At a glance it is possible to see that the overall efficiency of 405 nm light to promote the photolysis is the highest, the curve at 532 nm being the lowest.

As in neutral solutions the Rhodamine ligand exists in its spirolactam form, all the absorption at the visible region occurs through the Ru-bpy ^{1}MLCT band. From the photolysis data the quantum yields of the photoprocess at the different conditions can be calculated. Given the power of the irradiation beam, its optical path, and the volume and concentration of the complex solution, the differential amount of product is

$$\frac{dn_P}{dt} = I_{beam}(1 - 10^{-Abs_T})\frac{Abs_R}{Abs_T}\varphi_P \quad (1)$$

where n_P are the moles of product, I_{beam} is the intensity of the incident light in Einsteins/s, Abs_T and Abs_R are the total solution's absorbance and the reactant's absorbance, respectively, and φ_P is the quantum yield of photolysis. The calculation was performed through a numerical integration of eq 1 using a finite differences algorithm in a simple spreadsheet (using solver) or a Quick Basic routine (simplex) from which the value of φ_P is fitted.

dx.doi.org/10.1021/jp504030f | J. Phys. Chem. A XXXX, XXX, XXX−XXX

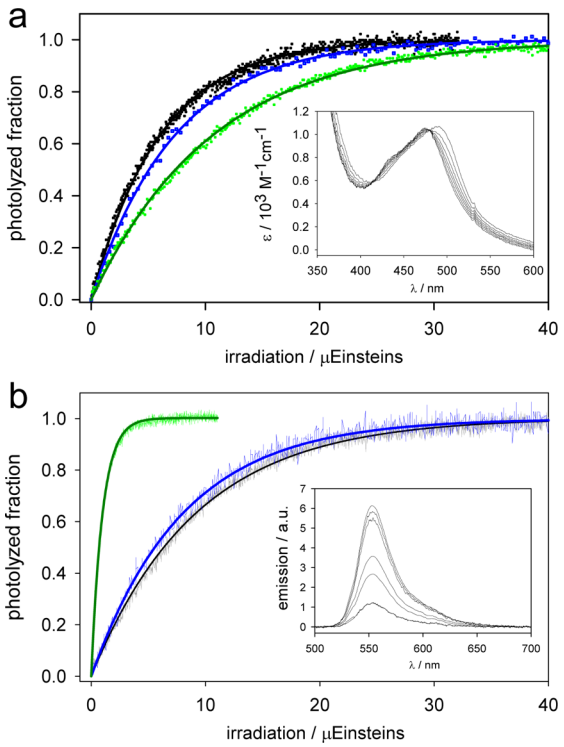

Figure 4. (a) Photolysis of solutions of $[Ru(bpy)_2(Rhod6G\text{-}4Pic)Cl]^+$ in EtOH/H_2O 70:30 v/v at three different wavelengths: from left to right 405, 445, and 532 nm. Inset: several absorption spectra during the photolysis at 532 nm. (b) Photolysis of solutions of $[Ru(bpy)_2(H\text{-}Rhod6G\text{-}4Pic)Cl]^{2+}$ EtOH/H_2O 70:30 v/v containing 10 mM of HTos at three different wavelengths: from left to right, 532, 445, and 405 nm. Inset: several fluorescence spectra during the photolysis at 532 nm. The solid lines are the best fits obtained integrating eq 1 (see text). Parameters: 405 nm laser, P = 8.37 mW (2.83×10^{-8} Einsteins/s), x-axis corresponds to 1413 s; 445 nm laser, P = 50 mW (1.86×10^{-7} Einsteins/s), x-axis = 215 s; 532 nm laser, P = 9.3 mW (4.14×10^{-8} Einsteins/s), x-axis = 966 s.

The obtained quantum yields for the photolysis in these conditions range from 2.5×10^{-2} to 3.2×10^{-2}, depending on the wavelength.

The same measurement can be done for solutions of the same complex in acidic solutions. In these conditions H-Rhod6G-4Pic is in its open form and its absorption reaches a maximum around 534 nm ($\varepsilon \cong 74000$ M^{-1} cm^{-1}). As this high absorptivity somewhat obscures the changes in the Ru-bpy spectra during photolysis, the reaction was followed directly through its fluorescence. The results are depicted in Figure 4b. While the slopes are lower at 405 and 445 nm, indicating a lower efficiency as compared with the results at neutral solution, the curve at 532 nm shows a dramatic increase in photon capture. At this wavelength the molar absorptivity of the ligand is much higher than that of the ^{1}MLCT band of Ru-bpy and therefore most of the photons are absorbed by the ligand.

The same analysis allows us to calculate the quantum yields of photoreaction in the presence of the absorbing fluorophore. Table 1 shows a summary.

The same behavior is present in the other members of the family studied, $[Ru(bpy)_2(Rhod6G\text{-}1,2DAE)Cl]^+$ and $[Ru(bpy)_2(Rhod6G\text{-}1,3DAP)Cl]^+$. In these cases, the pyridine linker is replaced by a diamine having 2 or 3 carbon chain lengths. As expected from the higher basicity of the amines with respect to the pyridine ligand, the corresponding spectra are 20 nm shifted toward lower energies. This increased basicity also implies that the Ru−N bond is somewhat stronger, and its photostability is even higher than that of the Rhodamine bearing a pyridine linker. A summary is presented in Table 2.

By comparison of the yields obtained in neutral solutions, where the photon directly populates the ^{1}MLCT band that eventually led to ligand exchange with the ones measured in acidic solutions, in which most of the photons are absorbed through the Rhodamine ligands, shows that direct irradiation on the ^{1}MLCT band is a more efficient way to promote photolysis at short wavelengths. The quantum yields at acidic solutions (Rhod* → ^{1}MLCT energy transfer) are about a half of those of the quantum yields in neutral solution (direct ^{1}MLCT irradiation). However, at the longest wavelength (532 nm) the molar absorptivity of the open form of Rhod6G-4Pic is around 20 times higher than that of the Ru band, and therefore, the overall efficiency (measured as the product $\varepsilon\varphi_P$) is more than 7 times higher, implying a huge enhancement of the characteristics of Ru-bpy complexes as photodeliverers of molecules.

As a second comparison, useful to separate the intrinsic effects of the pH on the photoactivity from the effect of the direct (MLCT)/indirect (Rhod ligand) capture of the photon, we have obtained the values of φ_P for the analogue complex $[Ru(bpy)_2(4PAA)Cl]^+$ (4PAA = 4 picolylacetylamide). This complex shares the same coordination group (picoline) but the fluorescent Rhodamine is replaced with an acetamide group. (Note that we have chosen to study the expelling of chloride ion, which does not present dissociation changes with pH. This allowed us to separate the effects that could arise from ligand recaptation. Other usual ligands that can be protonated, as amines, pyridines, etc., could show additional variation of φ_P with pH.)

The figures for photolyses at every wavelength, in neutral and acidic EtOH, are all very similar ($\varphi_P \cong 3 \times 10^{-2}$) and slightly higher than that of the $[Ru(bpy)_2(Rhod6G\text{-}4Pic)Cl]^+$ at neutral pH. This suggests that the key factor that determines the value

Table 1. Quantum Yield φ_P and Photolysis Efficiency $\varepsilon\varphi_P$ of the Complex $[Ru(bpy)_2(Rhod6G\text{-}4Pic)Cl]^+$ and Its Analogue Not Bearing a Fluorophore Ligand $[Ru(bpy)_2(4PAA)Cl]^+$ in Neutral and Acidic EtOH/H_2O 70:30 v/v, at Three Different Wavelengths

	405 nm		445 nm		532 nm	
	$\varphi_P \times 10^3$	$\varepsilon\varphi_P$ M^{-1} cm^{-1}	$\varphi_P \times 10^3$	$\varepsilon\varphi_P$ M^{-1} cm^{-1}	$\varphi_P \times 10^3$	$\varepsilon\varphi_P$ M^{-1} cm^{-1}
$[Ru(bpy)_2(Rhod6G\text{-}4Pic)Cl]^+$ neutral (closed Rhod)	31.9 ± 2.0	185	24.9 ± 2.6	187	25.7 ± 1.9	101
$[Ru(bpy)_2(H\text{-}Rhod6G\text{-}4Pic)Cl]^{2+}$ acid (open Rhod)	13.3 ± 0.9	83	9.4 ± 0.6	83	9.8 ± 0.6	727
$[Ru(bpy)_2(4PAA)Cl]^+$ neutral	33.7 ± 2.0	195	32.7 ± 4.4	246	28.4 ± 1.4	112
$[Ru(bpy)_2(4PAA)Cl]^+$ acid	37.6 ± 4.0	217	29.6 ± 4.5	223	32.5 ± 4.5	128

dx.doi.org/10.1021/jp504030f | J. Phys. Chem. A XXXX, XXX, XXX−XXX

Table 2. Quantum Yield φ_P Complexes $[Ru(bpy)_2(Rhod6G\text{-}1,2DAE)Cl]^+$ and $[Ru(bpy)_2(Rhod6G\text{-}1,3DAP)Cl]^+$ at 532 nm in Neutral and Acidic EtOH/H_2O 70:30 v/v

	$\varphi_P \times 10^3$		
	photolysis Cl^- (neutral, 532 nm)	photolysis Cl^- (acidic, 532 nm)	photolysis Rhod (acidic, 532 nm)
$[Ru(bpy)_2(Rhod6G\text{-}1,3DAE)Cl]^+$	33.9 ± 4.6	20.8 ± 3.1	0.0033 ± 0.0006
$[Ru(bpy)_2(Rhod6G\text{-}1,2DAP)Cl]^+$	30.3 ± 3.9	15.7 ± 4.3	0.0033 ± 0.0008

of the quantum yields is the energy transfer pathway and not the acidity of the medium, at least within the range studied.

From all these measurements the whole picture of the behavior of Ru-bpy complexes bearing fluorescent Rhodamine ligands appears: the quantum yields of photoreaction when the primary absorption operates through the ligand are about 0.4 times the yields corresponding to direct ^{1}MLCT absorption. This result, in agreement with previous findings,[27,28] indicates that the overall efficiency of energy transfer from Rhod ligand to the ^{3}MC dissociative state is less than unity. At least two reasons can be thought to be responsible for this energy loss: the energy transfer efficiency Rhod* → ^{1}MLCT is around 40% or the specific ^{1}MLCT state (or substates) that is populated through this indirect mechanism does not always lead to the loosening of the Ru−Cl bond.

Some insight on this question can be obtained by measuring the quenching of the ligand Rhod6G-4Pic due to the presence of the MLCT band of the Ru-bpy center in different situations. From the complete photolysis in acid EtOH of the complex $[Ru(bpy)_2(Rhod6G\text{-}4Pic)Cl]^+$ to yield the bis-aqua complex and free Rhod6G-4Pic, it is possible to determine the degree of primary energy transfer, considering that this is the only photophysical process that influences the quenching. On this basis, the fluorescence of the free ligand ($\varphi_F \cong 0.95$) decreases at least 55-fold ($\varphi_F \leq 0.018$) when it is coordinated to the chlorido complex. That means that the reverse FRET from the Rhod donor to the Ru-bpy acceptor in $[Ru(bpy)_2(Rhod6G\text{-}4Pic)Cl]^+$ is around 98% (almost ideal) and that the reduced yield of photoaquation would be due to a decay path that does not led to the proper symmetry of the ^{3}MC state populated after the FRET. Other possibilities, as an increased deactivation through nonradiative processes arising from the vibrational modes of the rather big Rhod6G-4Pic ligand, seem improbable given the fact that the complex bearing the closed form of the ligand does not exhibit this lower photoactivity.

Once having the big picture of fluorophore-enhanced photorelease, we performed density functional theory (DFT) electronic structure calculations in order to provide some insight into the electronic structure, the electronic spectroscopy, and the nature of the lower energy excited states. The use of (TD)DFT has given a clear insight into the rules that underlie the photochemistry of Ru-bpy complexes.[42−44] However, the modeling of asymmetric complexes of the form $[Ru(bpy)_2(L_1)(L_2)]^{n+}$ with L1 ≠ L2 has been barely studied.[45] As a starting point, the monocationic species $[Ru(bpy)_2(py)Cl]^+$ was chosen as the most simple Ru-polypyridine fragment related to the actual species explored in this article.

Geometry Optimization, Molecular Orbital Diagram, and Electronic Spectrum Analysis. A full geometry optimization in vacuo without any symmetry imposed constraints of this species rendered a Ru(II) center in a pseudo-octahedral environment comprising six N atoms and a chloride, represented in Figure 5a. The Ru−N bond distances at 2.15 Å for the py fragment, average of 2.08 Å for the bpy N

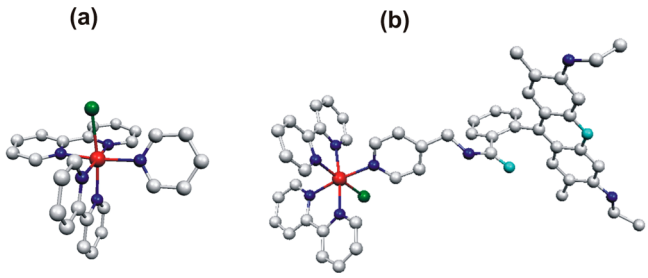

Figure 5. DFT optimized structures for the isolated cations (a) $[Ru(bpy)_2(py)Cl]^+$ and (b) $[Ru(bpy)_2(H\text{-}Rhod6G\text{-}4Pic)Cl]^{2+}$.

atoms, and the Ru−Cl bond length of 2.50 Å are within the expectations for this kind of system at this level of theory.[46−50]

The geometry resulting from a full optimization of $[Ru(bpy)_2(H\text{-}Rhod6G\text{-}4Pic)Cl]^{2+}$ is represented in Figure 5b. The metallic structural parameters are practically identical to those described for the simple pyridine derivative, and both Ru containing fragments can be virtually superimposed. The distance between the Ru center and the Rhodamine chomophore (measured from the geometric center of the latter) equals 12.2 Å

Figure 6a displays a MO diagram obtained from the DFT computations, which help to establish the electronic structure for the model compound. The low symmetry of the ligand environment lifts the d-orbital degeneracy, yielding three d_p orbitals of different energy. The HOMO and HOMO − 1 are mostly the d_{xz} and d_{yz} metal orbitals slightly destabilized (0.39 and 0.24 eV, respectively) with respect to the d_{xy} orbital due to the π-donating capability of the chloride. The LUMO is 2.86 eV above the HOMO. This orbital as well as the LUMO + 1 at 3.06 eV are located on the different bpy fragments. The lowest energy π^* orbitals of the less acceptor py shows up as the higher energy LUMO + 3. Finally the e_g^* set is represented by the LUMO + 9 d_z^2 and LUMO + 11 $d_{x^2-y^2}$ molecular orbitals sitting at 5.3 and 5.8 eV above the HOMO, respectively.

Figure 6b shows the MO diagram obtained for $[Ru(bpy)_2(Rhod6G\text{-}4Pic)Cl]^{2+}$. The presence of a rhodamine derivatized pyridine fragment introduces several molecular Rhodamine-centered molecular orbitals without any significant perturbation of the MO pattern on the metallic fragment. The linker between the different parts of the molecule does not allow for any electronic communication between fragments resulting in an electronic description that virtually can be decomposed into "metal-" and "Rhod-centered" MOs. The agreement in this case is very good and within the expectations for the level of theory employed for the computations. The high intensity band observed at 534 nm is predicted at 468 nm and assigned to the Rhod-centered intraligand $\pi-\pi^*$ transition. The theory suggests that the absorption pattern originating in the metallic chromophore remains virtually identical to the one in $[Ru(bpy)_2(py)Cl]^+$ except for a very small shift due to the substituent on the py ligand.

dx.doi.org/10.1021/jp504030f | J. Phys. Chem. A XXXX, XXX, XXX−XXX

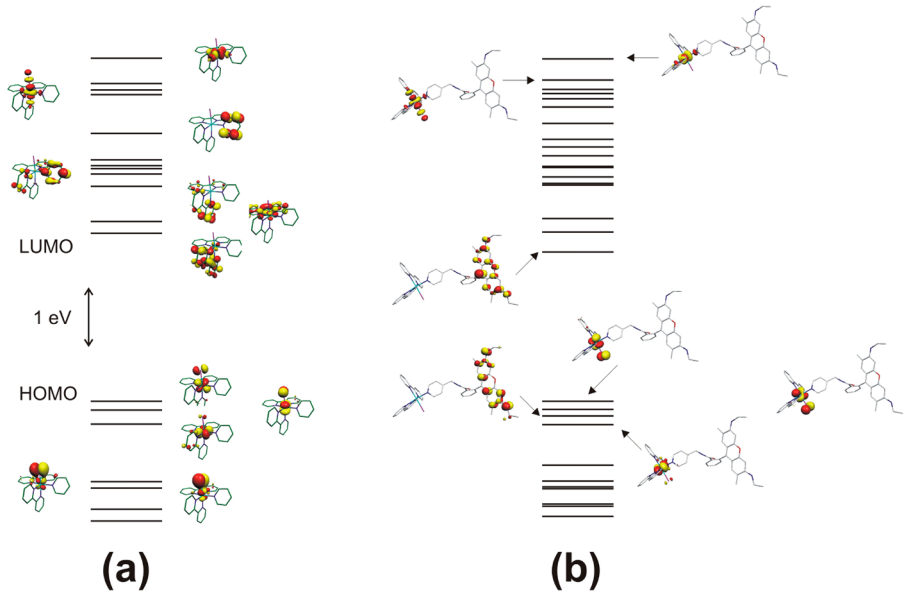

Figure 6. Molecular orbital diagram obtained from for the DFT optimized geometry for (a) $[Ru(bpy)_2(py)Cl]^+$ and (b) $[Ru(bpy)_2(Rhod6G\text{-}4Pic)Cl]^{2+}$. In both cases the energies refer to the HOMO level.

Figure 7 shows the (TD)DFT computed spectrum overlaid to the actual experimental one. A complete list of the computed transition energies, intensities, and orbital description as obtained from (TD)DFT can be found in the Supporting Information. The agreement is excellent, suggesting that the electronic picture described by the theory represents the actual physics of the system and therefore validating the theoretical approach. The computations show that the absorption observed in the visible region of the spectrum originates in metal-to-ligand CT transitions involving the different dπ and bpy* orbitals. The energy and the shape of the spectrum is well reproduced by the computations, including a noticeable tail to the low energy side of the spectrum arising from transitions that involve poorly overlapping metal and ligand orbitals.

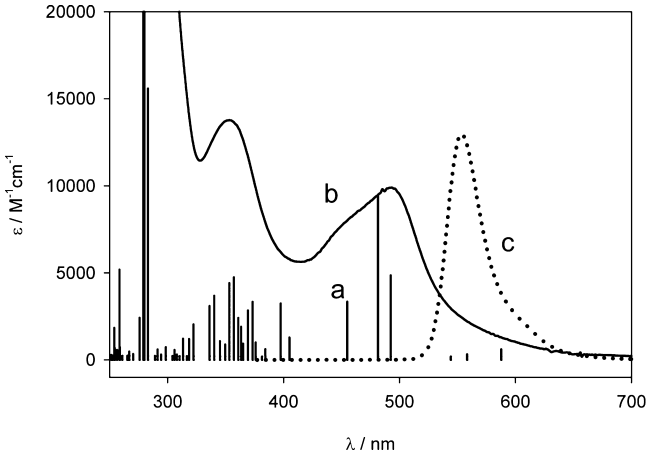

Figure 7. (a) Transitions calculated corresponding to the model complex $[Ru(bpy)_2(Py)Cl]^+$ in a medium of dielectric constant equal to that of EtOH/H_2O 70:30 v/v. (b) Experimental spectrum of $[Ru(bpy)_2(Rhod6G\text{-}4Pic)Cl]^+$ in EtOH/H_2O 70:30 v/v. (c) Fluorescence spectrum of coordinated Rhod6G-4Pic in HTos 10 mM EtOH/H_2O 70:30 v/v.

The overlap with the emission spectrum (Figure 7c) shows that some of the low-energy transitions from the tail of the spectrum could be important for the energy transfer from Rhodamine.

The order of magnitude of the expected energy transfer efficiency can be obtained from the FRET equations set.

$$\Phi_{FRET} = \frac{1}{1 + (r/R_0)^6} \tag{2}$$

$$\frac{R_0}{\text{nm}} = 0.02108\left[\frac{\kappa^2\Phi_f}{n^4}\left(\frac{J}{\text{mol}^{-1}\,\text{dm}^3\,\text{cm}^{-1}\,\text{nm}^4}\right)\right]^{1/6} \tag{3}$$

$$J = \int f_D(\lambda)\varepsilon_A(\lambda)\lambda^4 d\lambda \tag{4}$$

where Φ_{FRET} is the FRET efficiency, r the distance between donor (D) and acceptor (A), R_0 the characteristic distance of the D−A pair, κ^2 the dipole orientation factor, Φ_f the quantum yield of fluorescence of the donor in absence of the acceptor, n the refractive index of the medium, f_D the normalized (area = 1) donor emission spectrum, ε_A the acceptor molar absorptivity spectrum, λ the wavelength in nm, and J the superposition integral of donor emission and acceptor absorption spectra.

From the minimized structure obtained from DFT calculations we estimated the D−A distance to 12 Å. However, as the Rhodamine part of the ligand Rhod6G-4Pic can possibly rotate around its aliphatic carbon−carbon bond at 4 in the pyridine ring, κ^2 cannot be determined, and the usual value of 2/3 for free movement was used. The overlap between D emission and A absorption is scarce, given that the maximum of D emission, corresponding to Rhod6G-4Pic ligand, is red-shifted. This gives a moderately low value of the integral $J = 6.7 \times 10^{13}$ M^{-1} cm^{-1} nm^4 that corresponds to a characteristic $R_o \cong 3$ nm, quite small for a typical FRET. However, as the distance between D and A is much shorter (1.2 nm), the efficiency for the energy transfer for the first step in the photochemical chain is around 0.99.

dx.doi.org/10.1021/jp504030f | J. Phys. Chem. A XXXX, XXX, XXX−XXX

CONCLUSIONS

We have studied the photochemical properties of complexes of the form $[Ru(bpy)_2(F)Cl]^{n+}$, with F being a coordinated fluorescent dye (Rhodamine-6G derivatives). In particular the absorption of photons through the dye led to photodecomposition of the extra ligand following the dissociative mechanism described originally by Pinnick and Durham.[16−18] The (TD)DFT calculations show that there is no interaction between the MO pattern of the fluorescent ligand and the Ru center. This strongly suggests that the energy transfer is given by proximity and not through Dexter mechanisms, being the fluorescent ligand is the donor and the $Ru(bpy)_2$ core is the acceptor. Although donor emission and acceptor absorption spectra present a low degree of overlap, due to the red-shifted emission, the close distance between them allows an excellent energy transfer efficiency, close to unity. The change of the linker used to coordinate the fluorescent ligand to the metal center did not appreciably change the energy transfer properties, also suggesting that the close range of donor and acceptor are well within the efficient distances. However, the higher basicity of the aliphatic amines as compared with pyridine causes an increase in the bond stability after irradiation, which is shown by the much lower value of photolysis quantum yield of Rhodamine (3.3×10^{-6} vs 1.7×10^{-5}). The use of the $Ru(bpy)_2$ core opens a variety of possibilities for enhanced photodelivery of molecules of interest.

ASSOCIATED CONTENT

Supporting Information

Absorption/emission spectra of Rhod6G-4Pic, Rhod6G-1,2EN, and Rhod6G-1,3DAP. Molar absorptivities of the used complexes at the irradiaton wavelengths. Complete description of DFT-computed MO orbitals, energies, and transitions for $[Ru(bpy)_2(H\text{-}Rhod6G\text{-}4Pic)Cl]^{2+}$ and $[Ru(bpy)_2(Py)Cl]^{+}$. This material is available free of charge via the Internet at http://pubs.acs.org.

AUTHOR INFORMATION

Corresponding Author

*(R.E.) Phone: +54 11 4576-3358. E-mail: rober@qi.fcen.uba.ar.

Notes

The authors declare no competing financial interest.

ACKNOWLEDGMENTS

This research was supported by the National Agency for Science and Technology Promotion, CONICET, and the University of Buenos Aires. R.E. and L.D.S. are members of CONICET.

REFERENCES

(1) O'Regan, B.; Grätzel, M. A Low-Cost, High-Efficiency Solar Cell Based on Dye-Sensitized Colloidal TiO_2 Films. *Nature* **1991**, *353*, 737−741.
(2) Grätzel, M. Photoelectrochemical Cells. *Nature* **2001**, *414*, 338.
(3) Morandeira, A.; López-Duarte, I.; O'Regan, B.; Martínez-Díaz, M.; Forneli, A.; Palomares, E.; Torres, T.; Durranta, J. R. Ru(II)-Phthalocyanine Sensitized Solar Cells: The Influence of Co-Adsorbents Upon Interfacial Electron Transfer Kinetics. *J. Mater. Chem.* **2009**, *19*, 5016−5021.
(4) Jin, Z.; Masuda, H.; Yamanaka, N.; Minami, M.; Nakamura, T.; Nishikitani, Y. Efficient Electron Transfer Ruthenium Sensitizers for Dye-Sensitized Solar Cells. *J. Phys. Chem. C* **2009**, *113*, 2618−2623.
(5) Badaeva, E.; Albert, V. V.; Kilina, S.; Koposov, A.; Sykora, M.; Tretiak, S. Effect of Deprotonation on Absorption and Emission Spectra of Ru(II)-bpy Complexes Functionalized with Carboxyl Groups. *Phys. Chem. Chem. Phys.* **2010**, *12*, 8902−8906.
(6) Garner, R. N.; Gallucci, J. C.; Dunbar, K. R.; Turro, C. [Ru(bpy)(2)(5-cyanouracil)(2)](2+) as a Potential Light-Activated Dual-Action Therapeutic. *Inorg. Chem.* **2011**, *50* (19), 9213−9215.
(7) Zayat, L.; Calero, C.; Albores, P.; Baraldo, L.; Etchenique, R. A New Strategy for Neurochemical Photodelivery: Metal−Ligand Heterolytic Cleavage. *J. Am. Chem. Soc.* **2003**, *125*, 882−883.
(8) Zayat, L.; Salierno, M.; Etchenique, R. Ruthenium(II) Bipyridyl Complexes as Photolabile Caging Groups for Amines. *Inorg. Chem.* **2006**, *45*, 1728−1731.
(9) Zayat, L.; Noval, M. G.; Campi, J.; Calero, C. I.; Calvo, D. J.; Etchenique, R. A New Inorganic Photolabile Protecting Group for Highly Efficient Visible Light GABA Uncaging. *ChemBioChem* **2007**, *8*, 2035−2038.
(10) Filevich, O.; Etchenique, R. RuBiGABA-2: A Hydrophilic Caged GABA with Long Wavelength Sensitivity. *Photochem. Photobiol. Sci.* **2013**, *12*, 1565−70.
(11) Salierno, M.; Marceca, E.; Peterka, D. S.; Yuste, R.; Etchenique, R. A Fast Ruthenium Polypyridine Cage Complex Photoreleases Glutamate with Visible or IR Light in One and Two Photon Regimes. *J. Inorg. Biochem.* **2010**, *104*, 418−422.
(12) Filevich, O.; Salierno, M.; Etchenique, R. A Caged Nicotine with Nanosecond Range Kinetics and Visible Light Sensitivity. *J. Inorg. Biochem.* **2010**, *104*, 1248−1251.
(13) Araya, R.; Andino-Pavlovsky, V.; Yuste, R.; Etchenique, R. Two-Photon Optical Interrogation of Individual Dendritic Spines with Caged Dopamine. *ACS Chem. Neurosci.* **2013**, *4*, 1163−1167.
(14) Sun, Y.; Joyce, L. E.; Dickson, N. M.; Turro, C. Efficient DNA Photocleavage by $[Ru(bpy)_2(dppn)]^{2+}$ with Visible Light. *Chem. Commun.* **2010**, *46* (14), 2426−2428.
(15) Lunardi, C. N.; Cacciari, A. L.; Silva, R. S.; Bendhack, L. M. Cytosolic Calcium Concentration is Reduced by Photolysis of a Nitrosyl Ruthenium Complex in Vascular Smooth Muscle Cells. *Nitric Oxide* **2006**, *15*, 252−258.
(16) Pinnick, D. V.; Durham, B. Photosubstitution Reactions of $Ru(bpy)_2XY^{n+}$ Complexes. *Inorg. Chem.* **1984**, *23*, 1440−1443.
(17) Pinnick, D. V.; Durham, B. Temperature Dependence of the Quantum Yields for the Photoanation of $Ru(bpy)_2L_2^{2+}$ Complexes. *Inorg. Chem.* **1984**, *23*, 3841−3842.
(18) Durham, B.; Wilson, S. R.; Hodgson, D. J.; Meyer, T. J. Cis−Trans Photoisomerization in $Ru(bpy)^2(OH_2)_2^{2+}$. Crystal Structure of *trans*-$[Ru(bpy)_2(OH_2)(OH)](ClO_4)_2$. *J. Am. Chem. Soc.* **1980**, *102* (2), 600−607.
(19) Collin, J. P.; Jouvenot, D.; Koizumi, M.; Sauvage, J. P. Light-Driven Expulsion of the Sterically Hindering Ligand L in Tris-diimine Ruthenium(II) Complexes of the $Ru(phen)_2(L)_2^{2+}$ Family: A Pronounced Ring Effect. *Inorg. Chem.* **2005**, *44* (13), 4693−4696.
(20) Kramer, R. H.; Mourot, A.; Adesnik, H. Optogenetic Pharmacology for Control of Native Neuronal Signaling Proteins. *Nat. Neurosci.* **2013**, *16*, 816−823.
(21) Lee, H. M.; Larson, D. R.; Lawrence, D. S. Illuminating the Chemistry of Life: Design, Synthesis, and Applications of "Caged" and Related Photoresponsive Compounds. *ACS Chem. Biol.* **2009**, *4*, 409−427.
(22) Mayer, G.; Heckel, A. Biologically Active Molecules with a "Light Switch. *Angew. Chem., Int. Ed.* **2006**, *45*, 4900−4921.
(23) McCray, J. A.; Trentham, D. R. Properties and Uses of Photoreactive Caged Compounds. *Annu. Rev. Biophys. Biophys. Chem.* **1989**, *18*, 239−270.
(24) Wilcox, M.; Viola, R. W.; Johnson, K. W.; Billington, A. P.; Carpenter, B. K.; McCray, J. A.; Guzikowski, A. P.; Hess, G. P. Synthesis of Photolabile Precursors of Amino Acid Neurotransmitters. *J. Org. Chem.* **1990**, *55*, 1585−1589.

(25) Shembekar, V. R.; Chen, Y.; Carpenter, B. K.; Hess, G. P. A Protecting Group for Carboxylic Acids That Can Be Photolyzed by Visible Light. *Biochemistry* **2005**, *44*, 7107−7114.
(26) Fowles, G. R. *Introduction to Modern Optics*, 2nd ed.; Dover Publications: New York, 1989; Vol. *viii*, p 328.
(27) Filevich, O.; Garcia-Acosta, B.; Etchenique, R. Energy Transfer from a Rhodamine Antenna to a Ruthenium-Bipyridine Center. *Photochem. Photobiol. Sci.* **2012**, *11*, 843−847.
(28) Bahreman, A.; Cuello-Garibo, J. A.; Bonnet, S. Yellow-Light Sensitization of a Ligand Photosubstitution Reaction in a Ruthenium Polypyridyl Complex Covalently Bound to a Rhodamine Dye. *Dalton Trans.* **2014**, *43*, 4494−4505.
(29) Viala, C.; Coudret, C. An Expeditious Route to *cis*-Ru(bpy)$_2$C$_{12}$ (bpy = 2,2′-bipyridine) Using Carbohydrates as Reducers. *Inorg. Chim. Acta* **2006**, *359*, 984−989.
(30) Frisch, M. J.; et al. *Gaussian 09*, revision C.01; Gaussian, Inc.: Wallingford, CT, 2009.
(31) Becke, A. D. Density Functional Calculations of Molecular Bond Energies. *J. Chem. Phys.* **1988**, *84*, 4524−4529.
(32) Becke, A. D. Density-Functional Thermochemistry. III. The Role of Exact Exchange. *J. Chem. Phys.* **1993**, *98*, 5648−5652.
(33) Lee, C.; Yang, W.; Parr, R. G. Development of the Colle−Salvetti Correlation-Energy Formula into a Functional of the Electron Density. *Phys. Rev. B* **1988**, *37*, 785−789.
(34) Perdew, J. P. Density-Functional Approximation for the Correlation Energy of the Inhomogeneous Electron Gas. *Phys. Rev. B* **1986**, *33*, 8822−8824.
(35) Dunning, T. H., Jr.; Hay, P. J. Modern Theoretical Chemistry. In *Modern Theoretical Chemistry*; Schaefer, H. F., III, Ed.; Plenum: New York, 1976; pp 1−28.
(36) Hay, P. J.; Wadt, W. R. Ab Initio Effective Core Potentials for Molecular Calculations. Potentials for the Transition Metal Atoms Sc to Hg. *J. Chem. Phys.* **1985**, *82*, 270−283.
(37) Hay, P. J.; Wadt, W. R. Ab Initio Effective Core Potentials for Molecular Calculations. Potentials for K to Au Including the Outermost Core Orbitals. *J. Chem. Phys.* **1985**, *82*, 299−310.
(38) Wadt, W. R.; Hay, P. J. Ab Initio Effective Core Potentials for Molecular Calculations. Potentials for Main Group Elements Na to Bi. *J. Chem. Phys.* **1985**, *82*, 284−298.
(39) Woolley, P.; Steinhäuser, K. G.; Epe, B. Förster-Type Energy Transfer Simultaneous 'Forward' and 'Reverse' Transfer Between Unlike Fluorophores. *Biophys. Chem.* **1987**, *26*, 367.
(40) Adamczyk, M.; Grote, J. Efficient Synthesis of Rhodamine Conjugates through the 2′-position. *Bioorg. Med. Chem.* **2000**, *10*, 1539−1541.
(41) Kubin, R. F.; Fletcher, A. N. Fluorescence Quantum Yields of Some Rhodamine Dyes. *J. Lumin.* **1982**, *27*, 455−462.
(42) Salassa, L.; Garino, C.; Salassa, G.; Nervi, C.; Gobetto, R.; Lamberti, C.; Gianolio, D.; Bizzarri, R.; Sadler, P. J. Ligand-Selective Photodissociation from $[Ru(bpy)(4AP)_4]^{2+}$: a Spectroscopic and Computational Study. *Inorg. Chem.* **2009**, *48*, 1469−1481.
(43) Garino, C.; Salassa, L. The Photochemistry of Transition Metal Complexes Using Density Functional Theory. *Philos. Trans. R. Soc.* **2013**, *371*, 20120134.
(44) Petroni, A.; Slep, L.; Etchenique, R. Ruthenium(II) 2,2′-Bipyridyl Tetrakis-acetonitrile Undergoes Selective Axial Photocleavage. *Inorg. Chem.* **2008**, *47*, 951−956.
(45) Sizova, O. V.; Ershov, A. Y.; Ivanova, N. V.; Shashko, A. D.; Kuteikina-Teplyakova, A. V. Ru(II) Chloro-bis(bipyridyl) Complexes with Substituted Pyridine Ligands: Interpretation of Their Electronic Absorption Spectra. *Russ. J. Coord. Chem.* **2003**, *29*, 494−500.
(46) Li, J.; Noodleman, L.; Case, D. A. Electronic Structure Calculations with Applications to Transition Metal Complexes. In *Inorganic Electronic Structure and Spectroscopy*; Solomon, E. I., Lever, A. P. B., Eds.; Wiley: New York, 1999; Vol. *1*, pp 661−724.
(47) Roncaroli, F.; Ruggiero, M. E.; Franco, D. W.; Estiu, G. L.; Olabe, J. A. Kinetic, Mechanistic, and DFT Study of the Electrophilic Reactions of Nitrosyl Complexes with Hydroxide. *Inorg. Chem.* **2002**, *41*, 5760−5769.
(48) Videla, M.; Jacinto, J. S.; Baggio, R.; Garland, M. T.; Singh, P.; Kaim, W.; Slep, L. D.; Olabe, J. A. New Ruthenium Nitrosyl Complexes with Tris(1-pyrazolyl)methane (tpm) and 2,2′-Bipyridine (bpy) Coligands. Structure, Spectroscopy, and Electrophilic and Nucleophilic Reactivities of Bound Nitrosyl. *Inorg. Chem.* **2006**, *45*, 8608−8617.
(49) De Candia, A. G.; Marcolongo, J. P.; Etchenique, R.; Slep, L. D. Widely Differing Photochemical Behavior in Related Octahedral $\{RuNO\}^6$ Compounds: Intramolecular Redox Isomerism of the Excited State Controlling the Photodelivery of NO. *Inorg. Chem.* **2010**, *49*, 6925−6930.
(50) Osa Codesido, N.; De Candia, A. G.; Weyhermuller, T.; Olabe, J. A.; Slep, L. D. An Electron-Rich $\{RuNO\}^6$ Complex: *trans*-$[Ru(DMAP)_4(NO)(OH)]^{2+}$: Structure and Reactivity. *Eur. J. Inorg. Chem.* **2012**, *27*, 4301−4309.